

End-to-End Models for the Analysis of Pupil Size Variations and Diagnosis of Parkinson’s Disease

Dario Zanca^{1,*}, Alessandra Rufa¹, Andrea Canessa², and Silvio Sabatini²

¹DSMCN, University of Siena

²DIBRIS, University of Genova

^{*}Corresponding author: dario.zanca@unisi.it

Abstract

It is well known that a systematic analysis of the pupil size variations, recorded by means of an eye-tracker, is a rich source of information about a subjects cognitive state. In this work we present end-to-end models for the diagnosis of Parkinsons disease (PD) based on the raw pupil size signal. Long-range registration (10 minutes) of the pupil size were collected in scotopic conditions (complete darkness, 0 lux) on 21 healthy subjects and 15 subjects diagnosed with PD. 1-D convolutional neural network models are trained for classification of short-range sequences (10 to 60 seconds of registration). The model provides prediction with high average accuracy on a hold out test set. A temporal analysis of the model performance allowed the characterization of pupils size variations in PD and healthy subjects during a resting state. Dataset and codes are released for reproducibility and benchmarking purposes.

1 Introduction

While saccades and smooth pursuit allow us to direct the gaze towards a target of interest [6, 39], the eye also moves to adjust the amount of light that penetrates the bulb and reaches the lenses [32]. This movement can be registered as a variation of the pupil size. Pupils dilate and constrict in response to at least three different stimuli [18]: light, near fixations and increase in arousal and mental efforts. Scotopic experimental conditions [1] (i.e. complete darkness, 0 lux) minimize the first two factors and may be favourable to reveal fluctuations in pupil size that characterize certain cortical activity [36, 2, 10]. Several studies in literature propose methods for the analysis of the pupil size variations and for the characterization of this signal in isoluminant conditions or in the dark, with the goal of identifying patterns revealing changes in the cortical state activities. Under the assumption of non-linearity, common approaches usually

involve short-time Fourier or wavelets transformations [24, 25, 7, 29] to give a signal representation. These methods rely on an a priori choice of the basis function and tacitly assume stationarity of the phenomenon, which hardly hold for many biometric psychological signals [27, 28, 23]. Recently, some non-linear non-stationary approaches have been proposed that take advantage of projecting the pupil size signal in a frequency domain [35], in a latent space [20, 22], or their combination [26]. In all cases, basis curves are function of time and an *a posteriori* cross-correlation analysis allows to investigate hypotheses on the dynamic interactions among the systems modulating pupil size variations. These approaches are limited to a signal inspection that is difficult to extend to a more general modeling [41], do not deal with the wide variability between different subjects and are usually required to include a large number of pre-processing operations (blink removal, normalization, filtering, ...).

In this paper, we propose the learning of latent signal representations in a completely *data-driven* approach, by minimizing a classification error function. Differently from other approaches [26, 20, 22], we do not make use of *ad hoc* normalizations to reduce inter-subject variability *nor* for filtering noise, artifacts or outliers. Data pre-processing is limited to the interpolation with cubic splines on missing data. A normalization rule is learned in conjunction with the model, directly from data, by a properly defined normalization layer. We apply our method to the problem of diagnosing Parkinson’s disease. Making a reliable diagnosis is still an open-ended problem [3, 12] and therefore significant markers are sought that are able to characterize the disease, especially in its early stages [19]. For this reason new tools and evaluation procedures are needed in order to provide clinicians with more accurate and informative measurements and interpretation of symptoms. Scientific evidences underlie anomalies in PD patients pupil size regulation. Pupillary abnormalities have been observed [21] for Parkinson’s patients, even without overt clinical autonomic dysfunction [4] and during induced pupillary light reflex. Recent studies also demonstrate a reduced pupillary reward sensitivity connected to dysfunction in dopaminergic pathways [17]. This scientific evidence suggests that there exist distinctive pattern in the pupil diameter regulation activity among healthy subjects and PD patients.

The paper is organized as follows. In section 2 we provide a description of the learning model used for the task of classification of pupil signal sequences. Data collection protocol and experimental setup are discussed in section 3, together with some statistics of the collected data. In the same section we summarize model’s performance and compare them to the baselines. Finally, an in depth discussion of the results and suggestions for future works are given in section 4.

2 Method

We exploit 1-D convolutional neural network models [5, 14] (1D-CNN) for automatically extract effective features from the raw pupil size signal. Similar architectures are used in literature for similar problems involving the classifi-

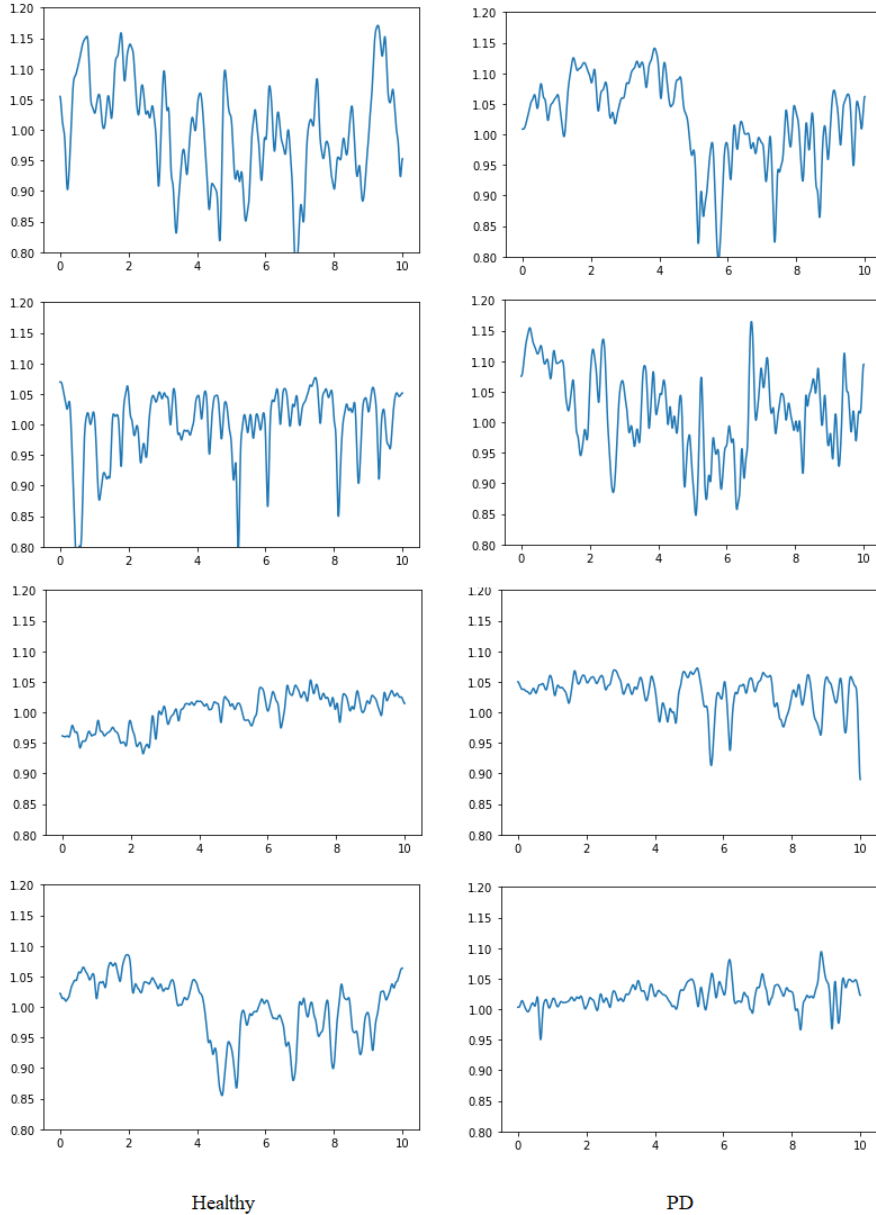


Figure 1: Examples of individual pupil signals. On the left-hand column, individual signals of healthy subjects. On the right-hand column, individual signals of PD patients. Diagnosis solely based on a visual inspection of this graphs is challenging even for an expert supervisor.

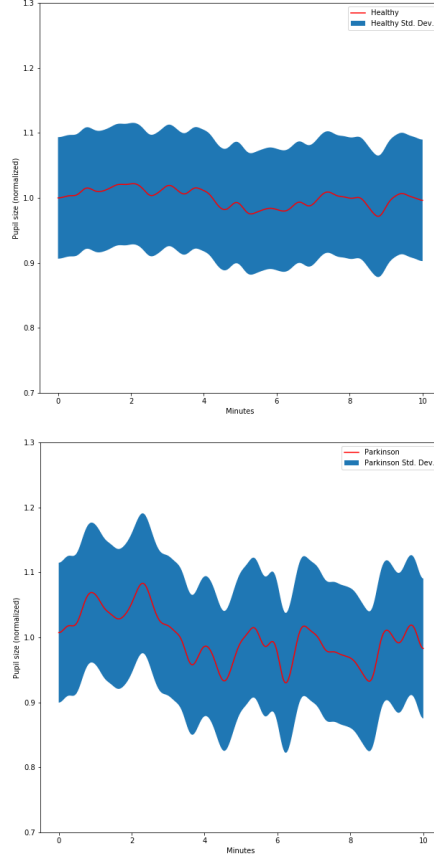


Figure 2: Pupil size signal. The two graphs show the normalized pupil size along the 10 minutes of the experiments.

cation of other biometric 1-dimensional signals. See, for example, application to Electrocardiogram (ECG) [11, 13, 15] or EEG [30, 34, 40].

Feature extraction consists of layers realizing convolutional and pooling operation. Convolutional layers can be seen as the application of filters that enhance some features of the original signal while reducing noise. Finally a non-linear activation function is applied. The output of a convolutional layer can be written as

$$x_j^l = \sigma \left(\sum_{i \in M_j} x_i^{l-1} * W_{i,j}^l + b_j^l \right),$$

where M_j represents the receptive field of the current unit, l is the layer index, $W_{i,j}^l$ are the parameters associated with the kernel applied and σ is the non-linear activation function chosen for the layer. We indicate with $*$ the convolutional operator. Differently by the multilayer perceptron (MLP), CNNs

gain both translation invariance due to the architecture of the model, which results favourable when searching for patterns in data that presents a known grid-like topology (time-series are a special case of 1-D grids). Pooling layers are intended to reduce the size of the input. This reduces the computational cost as well as inducing favourable properties to the learned functions, such as scale invariance [5].

Given the small amount of available data, we also introduce artificial noise by applying a dropout operation [33] to the input of the model. This is demonstrated to reduce the over-fitting by preventing complex co-adaptations on training data.

At the top of the convolutional module, a number of fully connected layers is added,

$$x_j^l = \sigma\left(\sum_i x_i^{l-1} W_j^l + b_j^l\right),$$

which allows learning non-linear combinations of the convolutional features. The best number of convolutional and fully connected layers has been validated experimentally (with grid search). Finally a softmax layer generates a 2-dimensional output for class prediction.

Normalization of the pupil size signal is often performed as pre-processing of the data, in order to reduce inter-subject variability [26, 20, 22]. In this work, we learn a normalization rule in conjunction with the neural model. This is done by introducing a normalization layer [9] before the convolutional module. Using of a normalization layer has been demonstrated to accelerate deep network training [31] by inducing a more predictive and stable behavior of the gradients.

3 Experiments

In this section, we present two main experimental contributions. First, we provide a dataset of registrations of pupil size variations in healthy subjects (HCs) and Parkinson’s patients (PDs), carried out under scotopic conditions (complete darkness) in order to minimize pupil reflexes due to light or near stimuli. Together with a description of the protocol adopted for the data collection, we also present a short sequence analysis together with two baselines for the classification. As a second contribution, we propose deep learning models for the classification of pupil size time-series that may be applied for diagnostics. Since deep learning models are learned to classify sequences consisting on a few seconds of recording (10 to 60 seconds), we show the scores in terms of prediction accuracy for different input lengths.

3.1 Data collection and pre-processing

The dataset contains the monocular pupil size recordings of 21 healthy subjects (HCs, average age 36 ± 13) and 15 patients diagnosed with Parkinson’s disease (PDs, average age 69 ± 7), for a total of 36 participants. HCs did not have neurological deficits or serious refractive problems. The pupil size recordings were acquired with an ASL 504 eye-tracker device (mean sampling frequency of

240 Hz). The distance of the camera from the participant’s eye is 650 mm. The participants head is kept still by means of a chinrest for the entire experimental session. Data is collected in a light-controlled setup in a scotopic condition (complete darkness, 0 lux measured) [1]. Participants are asked to look straight, minimize mental activity and relax. Participant pupil size is recorded for 11 minutes. The first minute of dark adaptation is discarded [38, 16]. Raw data is not filtered, nor normalized.

The difficulties introduced by the extreme experimental conditions and instrumental limits produce the undesired high presence of missing data within the recordings (average 8.47% of missing data per registration). They occur when the pupil size is undetectable in a certain time step, due to blinks or other factors. As a general rule [26, 20, 22], we interpolate missing data with cubic splines. However, we hypothesize that the Parkinson’s characteristic tremors may affect registration’s quality with patterns recognizable by the automatic learning algorithms. This would lead to erroneous conclusions of a link between the disease and pupil size. To address this problem, results will be given also for the case in which the dataset is modified by randomly superimposing the missing data patterns of one class to the other. This will be better explained in section 3.3.

3.2 Baselines

Here we try to identify coarse-grained trends within the two groups, i.e. HCs and PDs. Figure 2 shows the normative graphs of the pupil size signals for HCs and PDs, respectively. In order to compute normative graphs, pupil signals are normalized by dividing by the subject’s mean pupil size [26]. Normative plots present substantial differences that seem to indicate a visible difference between the two classes. However, individual signals show high variability and producing a diagnosis based of a visual exploration of the signal graph is a challenging task even for an expert supervisor. Some examples of individual signals can be observed in Figure 1. The left column shows four example graphs for PDs, while the right column shows the signal records for HCs. The task of identifying the correspondent class is not trivial and these examples suggest that differences should researched in complex combinations of signal features.

We define and evaluate two baseline models, based on the normative graphs, which will be compared with the model’s performance. For baseline *B1*, we calculate the Euclidean distance of the normalized pupil size signal from the normalized graphs. The sample is assigned to the class corresponding to the nearest normative graph. For the second baseline *B2* we compute the Kullback-Leibler divergence between two signals when viewed as distributions: it is a non-symmetric measure of the information lost when the normative graph is used as estimate of a given signal. Scores for the baselines are summarized in table 1.

Baseline	Accuracy
<i>B1</i>	63.89%
<i>B2</i>	61.11%

Table 1: **Baselines *B1* and *B2*.** Baseline *B1* is based on the Euclidean distance of the normalized pupil size signal from the normalized graphs. The sample is assigned to the class corresponding with the nearest normative graph. For the second baseline *B2* we compute the Kullback-Leibler divergence between two signals when viewed as distributions.

Layer (type)	Units
Batch norm.	Same as input
Dropout	–
Convolutional	$16F, 5 \times 1$
Pooling	2×1
Convolutional	$32F, 3 \times 1$
Flatten	–
Fully connected	$10 HU$
Softmax	2

Table 2: **1D-CNN architecture.** The best estimator structure has been selected with a grid search. It is composed by a batch normalization layer, two convolutional layers and a fully connected layer. A softmax layer on the top. F = "filters", HU = "hidden units".

3.3 Results

Pupil size registrations are divided into sub-sequences, each corresponding to n seconds of registration, with $n \in \{10, 15, 30, 60\}$. For the case of 10 and 15 seconds, we discard sequences that contain more than the 10% of missing data. For longer sequences of 30 and 60 seconds, we increase this threshold to 15% and 20% respectively. Sub-sequences are then shuffled inside each set. For each of the conditions, we perform a 5-fold cross validation. The recordings are randomly divided into 5 folds as follows: train (24 subjects), validation (6 subjects, balanced classes) and test sets (6 subjects, balanced classes). The folds are fixed in advance and the same folds are used for all trials. The folds configuration used in this paper is released together with the dataset for reproducibility purposes. We train the proposed 1D-CNNs models for a task of binary classification (i.e., healthy subjects vs. Parkinson's patients). We select a model architecture with a grid-search to identify the number of convolutional layers $n_c \in \{1, 2, 3\}$ and fully connected layers $n_{fc} \in \{1, 2, 3\}$. The best architecture for the task is defined in the table 2.

Table 3 shows mean accuracy and standard deviation in a 5-fold cross validation. In order to verify the effectiveness of the normalization layer, we

Model	Seq. len. (sec.)	Norm. (PP/BN)	Accuracy (%)
1D-CNN	10	PP	54.16(± 0.69)
1D-CNN	10	BN	75.84(± 1.25)
1D-CNN	15	PP	73.30(± 1.94)
1D-CNN	15	BN	83.67(± 0.29)
1D-CNN	30	PP	66.00(± 2.06)
1D-CNN	30	BN	75.14(± 0.97)
1D-CNN	60	PP	63.15(± 0.88)
1D-CNN	60	BN	75.20(± 1.88)

Table 3: **Accuracy on pupil signal classification.** Model performance are summarized in this table. The last column report the average accuracy score on the test set for a 5-fold cross validation. Standard deviation is between brackets. Two types of normalization have been evaluated: PP (pre-processing) scales data dividing the the subject’s mean pupil size, BP (batch normalization) learns normalization in conjunction with the network as a normalization layer. In bold, the best predictor’s score.

compare the performance with an identical 1D-CNN in which the normalization layer *BN* is substituted by a pre-processing operation *PP* of data normalization. In particular, sequences are re-scaled by dividing by the subject’s mean pupil size. Note, this corresponds to the procedure used to obtain the normative graphs in figure 2. Because of the high inter-subject variability (and scarceness of samples), the network is not able to perform in a comparable way without a parameterized and learnable normalization layer. In the best case (sequence length = 15 seconds, normalization = batch normalization layer), the proposed model overcome the diagnostic performance (82% accuracy) of the process described in [8], which is based on a complex set of clinical tests (both invasive and non-invasive) and interpretation by a human expert. The model’s best performance are obtained for 15-seconds sequences. This may find an explanation in the fact that longer sequences are more affected by the noise given by the missing data. Also, as the input dimensionality grows, so the feature space dimensionality does, while the size of the dataset decreases.

As already mentioned, the dataset contains a not negligible amount of missing data. Parkinson’s characteristic tremor may affect registration’s quality and produce patterns of noise which is recognizable by the automatic learning algorithms. Even if the signal is interpolated before being given as input to the model, some characteristic artifacts of the two groups may affect the signal. Although this does not limit the validity of the method for applicability and diagnosis purposes, it raises the doubt that the performance may be due to interwound characteristics of the instrument rather than to the specific properties of the pupil size. To verify that the classification is actually based on

Model	Seq. len. (sec.)	Norm. (PP/BN)	Accuracy (%)
1D-CNN	10	PP	54.20(± 1.56)
1D-CNN	10	BN	77.19(± 3.33)
1D-CNN	15	PP	74.65(± 1.08)
1D-CNN	15	BN	81.26(± 1.79)
1D-CNN	30	PP	56.67(± 1.77)
1D-CNN	30	BN	79.27(± 3.99)
1D-CNN	60	PP	59.99(± 3.99)
1D-CNN	60	BN	72.20(± 3.37)

Table 4: **Accuracy on pupil signal classification (mixed missing data).** Model performance are summarized in this table for the case of the dataset with mixed missing data. The last column report the average accuracy score on the test set for a 5-fold cross validation. Standard deviation is between brackets. Again, two types of normalization have been evaluated: PP (pre-processing) scales data dividing the the subject’s mean pupil size, BP (batch normalization) learns normalization in conjunction with the network as a normalization layer. In bold, the best predictor’s score.

patterns identified in the information carried out by the pupil size, we proceed by generating *mixed noise datasets*. Again, datasets are created for subsequences of different lengths. For each subsequence, we add a mask of missing data corresponding to another example of the dataset, randomly chosen from the complementary class. Each subsequence will then contain missing data points from both classes. Each example in the dataset contains, in this way, on average the same number and patterns of missing data. As usual, on those missing data points we interpolate with cubic splines. In this way, the classification must be based on the clean pupil size signal properties. Results are reported in table 4. Accuracy scores are comparable with the previous case, indicating that classifiers do not rely their decision on noise or signal’s artifacts.

We exploited sub-sequences instead of the long range signals for two main reasons: first, to provide the model with a consistent number of samples for the learning of the parameters; second, to obtain models capable of providing a temporal evaluation of the signal, i.e. finding out when the two signals (healthy and PD) diverge *most* during the 10-minutes-long exposure to complete darkness. To this second end, we leverage the best predictor to perform a time analysis of the pupil size signals during the whole duration of the long-range experiment (10 minutes in scotopic condition). The graph in the figure 3 shows the average accuracy at each instant of time, together with its standard deviation. This is obtained by evaluating the best predictor on all the sub-sequences of the test set. It should be noted that around the middle of the experimental session, performance considerably increases. While we report the graph only for the

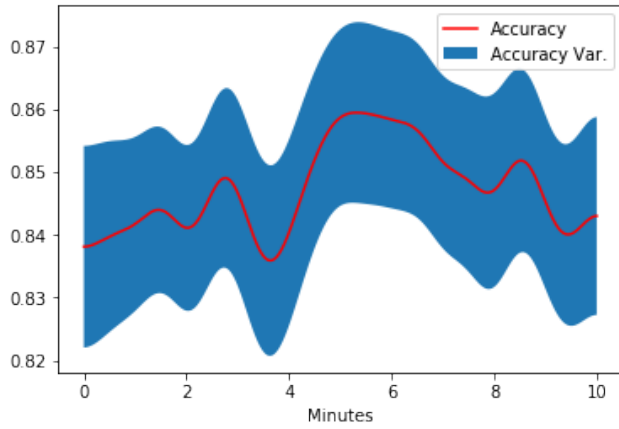


Figure 3: Accuracy of the best predictor. This graph illustrate the performance of the best predictor during the whole duration of the long-range experiment (10 minutes in scotopic condition), calculated averaging the scores on the test sets.

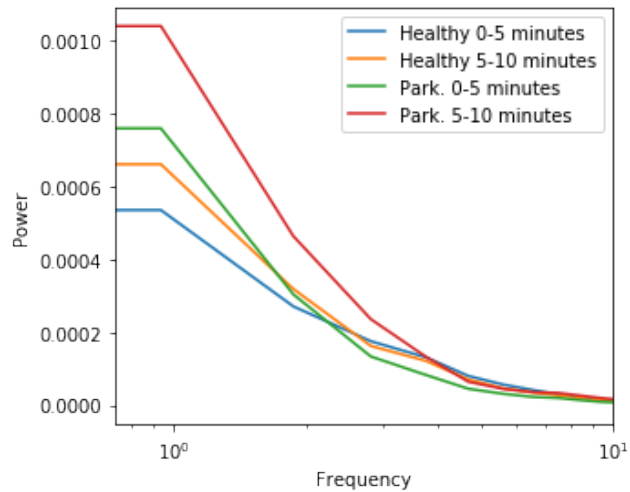


Figure 4: Power spectra. This graph illustrate the power spectrum in the first half (0-5 minutes) and in the second half (5-10 minutes) of the long range experiment for both populations (healthy control (HCs) and Parkinson's subjects (PDs)).

best predictor, the same trend has been observed for all classifiers. similarly trained. This phenomenon tells us that approximately from the minute 5 (equiv. minute 6, if we consider also the first minute of exposure to complete darkness, excluded from the dataset because of dark adaptation) of the experimental session, an inherent change on the pupil signal’s oscillation makes the PDs more easily distinguishable from HCs. For this reason we perform an analysis of the signals in the first half of the experiment (0-5 minutes) and in the second half (5-10 minutes) with the goal of identifying substantial differences among signals representation in the frequency domain. Figure 4 shows the power spectral density estimates, calculated using Welch’s method [37], for HCs and PDs in the two time windows. For HCs a significant change in the representation of the signal in the frequency domain can be observed. Low frequency power increases remarkably from the first half of the experiment to the second. This change is milder for PD patients. This fact provides us with a reasonable explanation of the change in the model’s performance.

4 Conclusion

In this paper we provide a twofold contribution. On the one hand, a dataset of raw pupil data of subjects in different clinical conditions (healthy, PD) together with a data collection protocol (scotopic) that enhances the contribution of cortical state activations to the pupil size variations. On the other hand, a tool for the automatic diagnosis of Parkinson’s disease using 1D-CNNs is learned from the data. In the best case ($83.67\% \pm 0.29\%$ accuracy), the proposed model overcome the diagnostic performance (82% accuracy) of a state-of-the-art complex set of clinical tests. The analysis of the model’s performance shows a change in the signal of the subjects around from the minute 5 of exposure to complete darkness.

Characteristic distributions in the frequency domain, analyzed in two different time ranges (0-5 minutes, 5-10 minutes), allowed pupil signal characterization. In order to develop more robust benchmarks and highly reliable diagnostic tools, it is necessary to expand the collected dataset. The procedure for collecting data under scotopic conditions seems promising and is highly recommended.

Future works may include learning long-term dependencies through the use of recurring architectures. To this end, larger amount of data needs to be collected. Since the data of healthy patients are more easily accessible, this would lead to very unbalanced datasets. However, techniques can be imported from the literature of novelty detection or few shot learning to extend the methodology proposed in this manuscript.

References

- [1] BH Crawford. The scotopic visibility function. *Proceedings of the Physical Society. Section B*, 62(5):321, 1949.

- [2] Andrew T Duchowski. Eye tracking methodology. *Theory and practice*, 328(614):2–3, 2007.
- [3] Douglas J Gelb, Eugene Oliver, and Sid Gilman. Diagnostic criteria for parkinson disease. *Archives of neurology*, 56(1):33–39, 1999.
- [4] Evangelia Giza, Dimitrios Fotiou, Sevasti Bostantjopoulou, Zoe Katsarou, and Anna Karlovasitou. Pupil light reflex in parkinson’s disease: evaluation with pupillometry. *International Journal of Neuroscience*, 121(1):37–43, 2011.
- [5] Ian Goodfellow, Yoshua Bengio, and Aaron Courville. *Deep learning*. MIT press, 2016.
- [6] Mary Hayhoe and Dana Ballard. Eye movements in natural behavior. *Trends in cognitive sciences*, 9(4):188–194, 2005.
- [7] David B Henson and Thomas Emuh. Monitoring vigilance during perimetry by using pupillography. *Investigative ophthalmology & visual science*, 51(7):3540–3543, 2010.
- [8] Andrew J Hughes, Susan E Daniel, Linda Kilford, and Andrew J Lees. Accuracy of clinical diagnosis of idiopathic parkinson’s disease: a clinicopathological study of 100 cases. *Journal of Neurology, Neurosurgery & Psychiatry*, 55(3):181–184, 1992.
- [9] Sergey Ioffe and Christian Szegedy. Batch normalization: Accelerating deep network training by reducing internal covariate shift. *arXiv preprint arXiv:1502.03167*, 2015.
- [10] Herbert E Ives. Critical frequency relations in scotopic vision. *JOSA*, 6(3):254–268, 1922.
- [11] Shweta H Jambukia, Vipul K Dabhi, and Harshadkumar B Prajapati. Classification of ecg signals using machine learning techniques: A survey. In *2015 International Conference on Advances in Computer Engineering and Applications*, pages 714–721. IEEE, 2015.
- [12] Joseph Jankovic. Parkinsons disease: clinical features and diagnosis. *Journal of neurology, neurosurgery & psychiatry*, 79(4):368–376, 2008.
- [13] Serkan Kiranyaz, Turker Ince, Ridha Hamila, and Moncef Gabbouj. Convolutional neural networks for patient-specific ecg classification. In *2015 37th Annual International Conference of the IEEE Engineering in Medicine and Biology Society (EMBC)*, pages 2608–2611. IEEE, 2015.
- [14] Yann LeCun, Léon Bottou, Yoshua Bengio, and Patrick Haffner. Gradient-based learning applied to document recognition. *Proceedings of the IEEE*, 86(11):2278–2324, 1998.

- [15] Dan Li, Jianxin Zhang, Qiang Zhang, and Xiaopeng Wei. Classification of ecg signals based on 1d convolution neural network. In *2017 IEEE 19th International Conference on e-Health Networking, Applications and Services (Healthcom)*, pages 1–6. IEEE, 2017.
- [16] Joseph Mandelbaum. Dark adaptation: some physiologic and clinical considerations. *Archives of Ophthalmology*, 26(2):203–239, 1941.
- [17] SG Manohar and M Husain. Reduced pupillary reward sensitivity in parkinsons disease. *npj Parkinson’s Disease*, 1(1):1–4, 2015.
- [18] Sebastiaan Mathôt. Pupillometry: Psychology, physiology, and function. *Journal of Cognition*, 1(1), 2018.
- [19] JOLYON Meara, BIMAL K Bhowmick, and Peter Hobson. Accuracy of diagnosis in patients with presumed parkinson’s disease. *Age and ageing*, 28(2):99–102, 1999.
- [20] L Mesin, A Monaco, and R Cattaneo. Investigation of nonlinear pupil dynamics by recurrence quantification analysis. *BioMed research international*, 2013, 2013.
- [21] G Micieli, P Tosi, S Marcheselli, and A Cavallini. Autonomic dysfunction in parkinson’s disease. *Neurological Sciences*, 24(1):s32–s34, 2003.
- [22] Annalisa Monaco, Ruggero Cattaneo, Luca Mesin, Edoardo Fiorucci, and Davide Pietropaoli. Evaluation of autonomic nervous system in sleep apnea patients using pupillometry under occlusal stress: a pilot study. *CRANIO®*, 32(2):139–147, 2014.
- [23] Yair Morad, Hadas Lemberg, Nehemiah Yofe, and Yaron Dagan. Pupillography as an objective indicator of fatigue. *Current eye research*, 21(1):535–542, 2000.
- [24] W Nowak, E Szul-Pietrzak, and A Hachol. Wavelet energy and wavelet entropy as a new analysis approach in spontaneous fluctuations of pupil size study–preliminary research. In *XIII Mediterranean Conference on Medical and Biological Engineering and Computing 2013*, pages 807–810. Springer, 2014.
- [25] Wioletta Nowak, Andrzej Hachol, and Henryk Kasprzak. Time-frequency analysis of spontaneous fluctuation of the pupil size of the human eye. *Optica Applicata*, 38(2), 2008.
- [26] Pietro Piu, Valeria Serchi, Francesca Rosini, and Alessandra Rufa. A cross-recurrence analysis of the pupil size fluctuations in steady scotopic conditions. *Frontiers in neuroscience*, 13:407, 2019.
- [27] Chi-Sang Poon and Christopher K Merrill. Decrease of cardiac chaos in congestive heart failure. *Nature*, 389(6650):492, 1997.

- [28] Francesca Regen, Hans Dorn, and Heidi Danker-Hopfe. Association between pupillary unrest index and waking electroencephalogram activity in sleep-deprived healthy adults. *Sleep medicine*, 14(9):902–912, 2013.
- [29] Jacob Reimer, Emmanouil Froudarakis, Cathryn R Cadwell, Dimitri Yatsenko, George H Denfield, and Andreas S Tolias. Pupil fluctuations track fast switching of cortical states during quiet wakefulness. *Neuron*, 84(2):355–362, 2014.
- [30] Subhrajit Roy, Isabell Kiral-Kornek, and Stefan Harrer. Chrononet: a deep recurrent neural network for abnormal eeg identification. In *Conference on Artificial Intelligence in Medicine in Europe*, pages 47–56. Springer, 2019.
- [31] Shibani Santurkar, Dimitris Tsipras, Andrew Ilyas, and Aleksander Madry. How does batch normalization help optimization? In *Advances in Neural Information Processing Systems*, pages 2483–2493, 2018.
- [32] Sylvain Sirois and Julie Brisson. Pupillometry. *Wiley Interdisciplinary Reviews: Cognitive Science*, 5(6):679–692, 2014.
- [33] Nitish Srivastava, Geoffrey Hinton, Alex Krizhevsky, Ilya Sutskever, and Ruslan Salakhutdinov. Dropout: a simple way to prevent neural networks from overfitting. *The journal of machine learning research*, 15(1):1929–1958, 2014.
- [34] Orestis Tsinalis, Paul M Matthews, Yike Guo, and Stefanos Zafeiriou. Automatic sleep stage scoring with single-channel eeg using convolutional neural networks. *arXiv preprint arXiv:1610.01683*, 2016.
- [35] Fabiola M Villalobos-Castaldi, Nicolás C Kemper-Valverde, Silvia Raquel García, and José Ruiz-Pinales. Pupillometric-based analysis of central autonomic levels using hht. In *2016 International Conference on Mechatronics, Electronics and Automotive Engineering (ICMEAE)*, pages 14–19. IEEE, 2016.
- [36] Nicholas A Webb and Michael J Griffin. Eye movement,vection, and motion sickness with foveal and peripheral vision. *Aviation, space, and environmental medicine*, 74(6):622–625, 2003.
- [37] Peter Welch. The use of fast fourier transform for the estimation of power spectra: a method based on time averaging over short, modified periodograms. *IEEE Transactions on audio and electroacoustics*, 15(2):70–73, 1967.
- [38] JM Woodhouse and FW Campbell. The role of the pupil light reflex in aiding adaptation to the dark. *Vision research*, 15(6):649–653, 1975.
- [39] Alfred L Yarbus. *Eye movements and vision*. Springer, 2013.

- [40] Özal Yıldırım, Ulaş Baran Baloglu, and U Rajendra Acharya. A deep convolutional neural network model for automated identification of abnormal eeg signals. *Neural Computing and Applications*, pages 1–12, 2018.
- [41] Alexandre Zénon. Time-domain analysis for extracting fast-paced pupil responses. *Scientific reports*, 7(1):1–10, 2017.